Proceedings of GT2006
ASME Turbo Expo 2006: Power for Land, Sea and Air
May 8-11, 2006, Barcelona, Spain

GT2006-90596

VIBRATION REDUCTION INVESTIGATION OF A SQUEEZE FILM DAMPER WITH VALVULAR METAL RUBBER

Ma Yanhong Hong Jie Deng Yin

School of Jet Propulsion, Beijing University of Aero. and Astro.

Mail Address: 405 Group, Bei-Hang, Beijing 100083, P.R. China;

Tel: +86-10-82338172; E-mail Address: **mayanh2002@sip.buaa.edu.cn**

ABSTRACT

A new-style squeeze film damper with valvular metal rubber squeeze film ring (SFD/VMR) was designed to improve characteristics of the squeeze film force of the SFD. The immobile squeeze film ring of the SFD was replaced by the elastic squeeze film ring with the valvular metal rubber subassembly (VMR). When the unbalance force was smaller, the displacement of the journal changed little, and then the squeeze film force was smaller too, so as to the squeeze film ring of the SFD/VMR was nearly immobile. The working condition was similar with the SFD. When the unbalance force was larger, the displacement of the journal changed bigger, and then the squeeze film force rapidly increased, so as to the VMR deformed, which made the film thickness changed correspondingly, until it reached a balanceable state of the squeeze film force and elastic force of the VMR.

Theoretical and experimental investigations showed that the SFD/VMR had optimal effect on reducing vibration, comparing with the SFD, because it could passively adjust the squeeze film clearance by taking advantage of the elastic deformation of the VMR. The SFD/VMR could control the squeeze film clearance in a suitable range, which made the characteristics of the squeeze film force of the SFD/VMR better than the SFD. The SFD/VMR could suppress the occurrence of the nonlinear vibration phenomenon markedly, such as bistable jump up.

NOMENCLATURE

C,c	radial clearance of damper
R, R_j	radius of damper journal
R_b	radius of squeeze film ring
L	damper journal width
m	equivalent mass of the rotor system
Q	unbalance
U	$=Q/mc$ unbalance parameter
d_s	wire diameter
μ	fluid absolute viscosity
ρ	oil density
k_s	stiffness of Squirrel Cage
ω_c	$=\sqrt{k_s/m}$ undamped critical speed of rotor
ω	rotor speed
δ	$=\dot{\phi}_j/\omega_c$ Speed parameter
B	$=\mu R_j L^3/(c^3 m\omega_c)$ bearing parameter,
O_j	center of journal
O_b	center of squeeze film ring
O_1	center of bearing seat
e_m	$=UC=Q/m$ eccentric distance of mass
e_j	eccentric distance of journal

e_b	eccentric distance of squeeze film ring
e	relative eccentric distance
ε_j	$=e_j/c$ eccentricity ratio of journal
ε_b	$=e_b/c$ eccentricity ratio of squeeze film
ε	$=e/c$ relative eccentricity ratio
ϕ_j	circumferential angle of journal
ϕ_b	circumferential angle of squeeze film ring
ϕ	relative circumferential angle
θ	circumferential angle
$P(x,z)$	local pressure within the squeeze film
P_r	radial film force
P_t	tangential film force
h	$=c(1+\varepsilon\cos\theta)$ film thickness
$h_{\_\min}$	least film thickness
H	$=h_{\_\min}/R_j$ dimensionless least film thickness
k_0	$=-P_r/e$ squeeze film Stiffness
d_0	$=-P_t/(e\Omega)$ squeeze film Damping
d_0/k_0	the ratio of damping to stiffness of squeeze film
k_b	stiffness of the VMR
η	loss coefficient of the VMR
d_b_ξ	$=\eta/2$ damping coefficient of the VMR
K_b	$=k_b/k_s$ dimensionless stiffness of the VMR
D_b	$=d_b\omega_c/k_s$ dimensionless damping of the VMR

1 INTRODUCTION

Squeeze film dampers (SFD) [1] were used extensively in modern gas turbine engines and other high-speed rotating machineries. However, the conventional SFD had some shortcomings that were difficult to overcome. If the unbalance force of a rotor system was too large, the squeeze film force presented high nonlinearity with the increase of the relative eccentricity ratio (Actually, the film thickness in the squeeze direction decreased.). It could cause nonlinear vibration of the rotor system such as bistable jump up.

In order to overcome above shortcomings, many scholars have made a lot of researches to improve the characteristics of squeeze film force of SFD and to extend the using range, on the basis of the keeping and developing the advantages of SFD. And many achievements have been accomplished[2-9].

Zhang Shiping and Yan Litang developed porous squeeze film damper (PSFD) [2] since 1989. Yet these holes were easy to block up because of the impure oil. Therefore, it wasn't used extensively.

D. P. Fleming developed duel clearance squeeze film damper (DCSFD) [3] since 1985. H.Hooshang and J.F.Waltton developed spiral foil multi-squeeze film damper (SFMSFD) [4] since 1991. But DCSFD and SFMSFD need the high-level manufacturing engineering.

Hybrid Squeeze Film Damper (HSFD) [6] were put forward successively by Zhu Changsheng and Wang Xixuan, but HSFD was hard to use in aeroengine due to the complicated structures.

Metal Rubber was a new and high-effective damper, which was made through the courses of selection of material, enwinding, prolongation, knit and mold pressing. It was called Metal Rubber, because it was made of metal material, and it had the quality that was similar with the rubber. At the same time, it had a lot of advantages such as the regulative stiffness, the high loss coefficient, the light weight, the strong adaptability of condition (be able to endure the high and low temperature and corrosion, anti-aging), and easy-making complex shape. It also possessed the better absorptive capability to the transient shock. Therefore, it could be used in many fields such as aviation, spaceflight, vessel, traffic transportation and architecture, etc.

For the direct application of metal rubber (it is called metal mesh in America) as a bearing damper, very few publications could be found. Zarzour and Vance [10] showed the insensitivity of metal mesh bearing dampers to high temperature and lubrication. Their work also investigated the effect of different interference fits on the stiffness and damping of metal mesh and suggested the viability of a hysteretic model. The furthered investigation of Al-Khateeb and Vance[11] showed that the parallel arrangement of the copper mesh damper with a squirrel cage forms a promising alternative to squeeze film dampers with comparable damping and many other desired features.

2 STRUCTURE DESIGN OF SFD/VMR

The structures of SFD and SFD/VMR were showed in Fig.1, and a structure of the VMR in Fig.2. The VMR consisted of VMR's inner ring(squeeze film ring), terminal cap of the inner ring, valvular metal rubber, VMR's outer ring, terminal cap of the outer ring, axial gasket and seating, as shown in Fig.1. In the radial direction, valvular metal rubber was in the middle of inner ring and outer ring of VMR. The structure was tight fit. In the circumferential direction, a set of bosses was designed to fix circumferential orientation in inner ring and outer ring of VMR. The number of the bosses was designed referred to the performance of the rotor system. In the axis direction, one side of inner ring and outer ring of VMR had boss, the other side fit with the terminal cap. By adjusting the thickness of the axial gasket, preload in the axis direction could be altered, which led to change the stiffness and damping characteristics of the valvular metal rubber. Assemble VMR(see Fig.2) was fixed in Bearing seat by bolt.

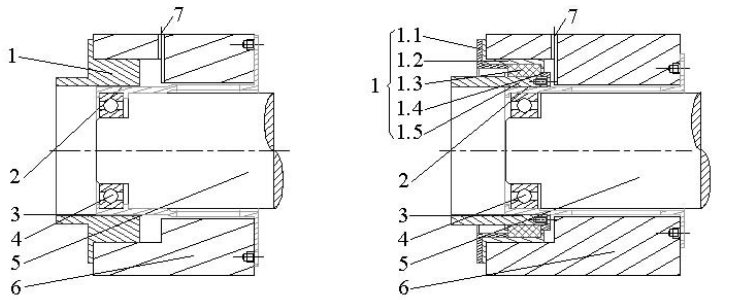

ITEM	DESCRIPTION
1	Oil Film Ring
2	Journal (Squirrel Cage)
3	Squeeze Film
4	Bearing
5	Shaft
6	Bearing Seat
7	Oiling Hope

ITEM	DESCRIPTION
1	Valvular Metal Rubber subassembly
1.1	Terminal Cap of Outer Ring of MR
1.2	Outer Ring of MR
1.3	Valvular Metal Rubber
1.4	Oil Film Ring (Inter Ring of MR)
1.5	Terminal Cap of Inter Ring of MR
2	Journal (Squirrel Cage)
3	Squeeze Film
4	Bearing
5	Shaft
6	Bearing Seat
7	Oiling Hope

Fig.1 The structure of SFD and SFD/VMR

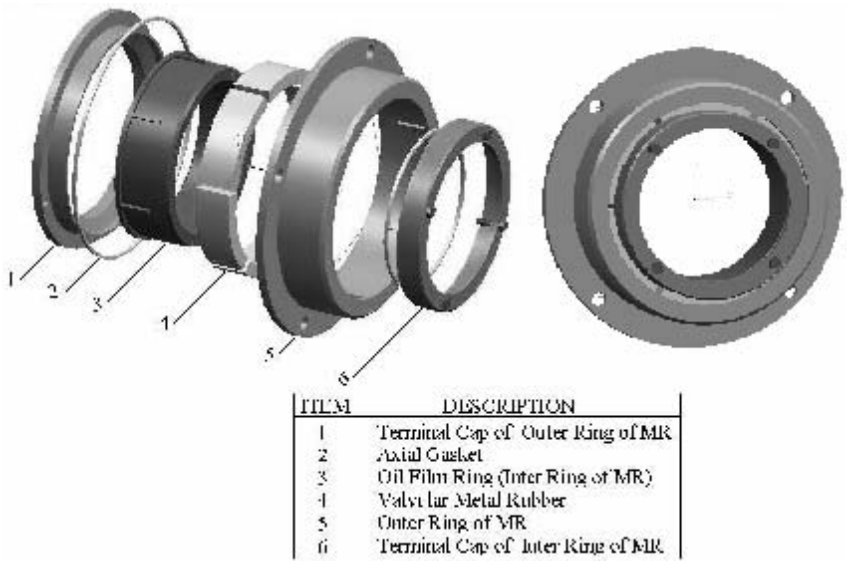

ITEM	DESCRIPTION
1	Terminal Cap of Outer Ring of MR
2	Axial Gasket
3	Oil Film Ring (Inter Ring of MR)
4	Valvular Metal Rubber
5	Outer Ring of MR
6	Terminal Cap of Inter Ring of MR

Fig.2 The structure of VMR

3 THEORETICAL ANALYSIS

The physical model of SFD/VMR was built on analysis of the dynamic forces and motion. The Reynolds equation of SFD/VMR was deduced, in the light of the N-S equation and the fluid continuity equation. Thus the characteristics of squeeze film force were solved.

3.1 Reynolds Equation of the SFD/VMR

Fig.3 showed the SFD/VMR's physical model with coordinates defined. Dashed indicated initial position of the damper. The stationary coordinates systems were established by $O_1\xi\eta Z$. Assuming metal rubber only deformed in the radial direction. The active coordinates systems *OXYZ* were built. The *X*-axis pointed to the circumferential direction of the journal surface. *Y*-axis pointed to the normal direction of the journal surface. *Z*-axis pointed to the axis direction of the journal. θ was the circumferential angle that started with the maximum film thickness.

It was assumed that the polar coordinates of the center of the squeeze film ring was $O_b(e_b,\phi_b)$, the eccentricity ratio of squeeze film ring was defined here as $\varepsilon_b = e_b / c$ the polar

coordinates of the center of the journal was $O_j(e_j,\phi_j)$, the eccentricity ratio of journal was defined here as $\varepsilon_j=e_j/c$. Moreover, assume the squeeze film pressure was *p(x, z)*. The film thickness *h* at any given location was given by $h=c(1+\varepsilon\cos\theta)$. The eccentricity displacement between O_j and O_b was *e*. The relative eccentricity ratio was defined here as $\varepsilon=e/c$.

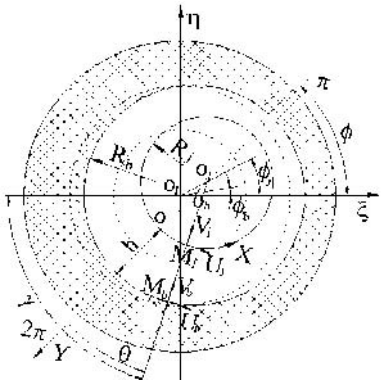

Fig.3 Physical model of SFD/VMR

The predigesting N-S equations [12] were integrated twice. And the boundary conditions were introduced

$$\left.\begin{array}{l} y=0 \text{ 时, } u=U_j, v=V_j, w=W_j=0 \\ y=h \text{ 时, } u=U_b, v=V_b, w=W_b=0 \end{array}\right\} \quad (1)$$

The speed of oil was obtained,

$$\begin{cases} u=\dfrac{1}{2\mu}\dfrac{\partial p}{\partial x}y(y-h)+\dfrac{U_b-U_j}{h}y+U_j \\ w=\dfrac{1}{2\mu}\dfrac{\partial p}{\partial z}y(y-h) \end{cases} \quad (2)$$

Oil motion had to be satisfied with a continuity equation, then

$$\frac{\partial\rho}{\partial t}+\frac{\partial(\rho u)}{\partial x}+\frac{\partial(\rho v)}{\partial y}+\frac{\partial(\rho w)}{\partial z}=0 \quad (3)$$

Substituting Eq. (2) into Eq. (3), integrating it, yielded,

$$\frac{\partial}{\partial x}(h^3\frac{\partial p}{\partial x})+\frac{\partial}{\partial z}(h^3\frac{\partial p}{\partial z})=6\mu(U_j-U_b)\frac{\partial h}{\partial x}+12\mu(V_b-V_j) \quad (4)$$

Taking into consideration the Fig.4, obtained,

$$\begin{aligned} U_j &= \dot{e}_j\sin(\theta+\phi-\phi_j)-e_j\dot{\phi}_j\cos(\theta+\phi-\phi_j) \\ V_j &= -\dot{e}_j\cos(\theta+\phi-\phi_j)-e_j\dot{\phi}_j\sin(\theta+\phi-\phi_j) \\ U_b &= \dot{e}_b\sin(\theta+\phi-\phi_b)-e_b\dot{\phi}_b\cos(\theta+\phi-\phi_b) \\ V_b &= -\dot{e}_b\cos(\theta+\phi-\phi_b)-e_b\dot{\phi}_b\sin(\theta+\phi-\phi_b) \end{aligned}$$

If $\gamma=\theta+\phi$, then $\theta=\gamma-\phi$, yielded,

$$\begin{aligned} U_j-U_b &= \dot{e}\sin\theta-e\Omega\cos\theta \\ V_b-V_j &= \dot{e}\cos\theta+e\Omega\sin\theta=\frac{\partial h}{\partial t}-\Omega\frac{\partial h}{\partial\theta} \end{aligned} \quad (5)$$

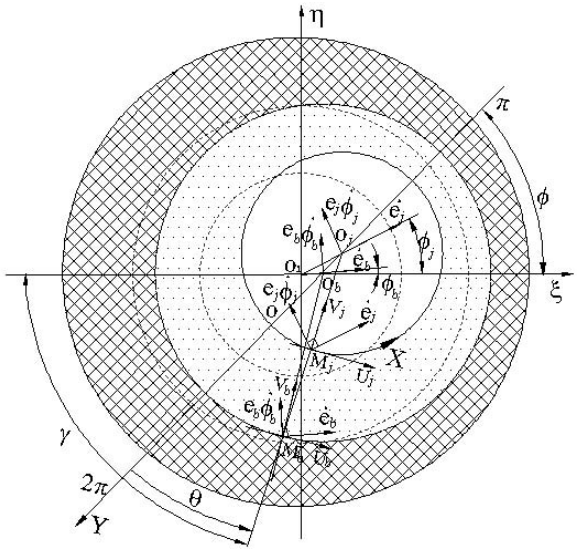

Fig.4 Speed relation of SFD/VMR

Substituting Eq. (5) into the Eq. (4), yielded,

$$\frac{1}{R_j^2}\frac{\partial}{\partial\theta}(h^3\frac{\partial p}{\partial\theta})+\frac{\partial}{\partial z}(h^3\frac{\partial p}{\partial z})=-12\dot{\phi}\mu\frac{\partial h}{\partial\theta}+12\mu\frac{\partial h}{\partial t} \quad (6)$$

This was the transient-state Reynolds equation of constant-viscosity incompressible fluid.

While the steady-state Reynolds equation of the SFD/VMR is,

$$\frac{1}{R_j^2}\frac{\partial}{\partial\theta}(h^3\frac{\partial p}{\partial\theta})+\frac{\partial}{\partial z}(h^3\frac{\partial p}{\partial z})=-12\mu\Omega\frac{\partial h}{\partial\theta} \quad (7)$$

a short bearing approximation[13] to the steady-state Reynolds equation (7) is

$$p(\theta,z)=-\frac{6\mu\Omega C\varepsilon\sin\theta}{h^3}(\frac{L^2}{4}-z^2) \quad (8)$$

By comparing the short bearing approximations of the SFD and SFD/VMR, we could know that they had a completely same form, but the two ε were different. The difference was as follows: the journal and squeeze film ring of SFD/VMR were mobile, ε was given by $\vec{\varepsilon}=\overrightarrow{\varepsilon_j}-\overrightarrow{\varepsilon_b}$. The squeeze film pressure of SFD/VMR was not only subject to $\vec{\varepsilon}_j$ and $\dot{\vec{\varepsilon}}_j$ but also the $\vec{\varepsilon}_b$ and $\dot{\vec{\varepsilon}}_b$. The squeeze film ring of SFD was fixed on the seating, namely $\vec{\varepsilon}_b=\vec{0}$, so $\vec{\varepsilon}=\overrightarrow{\varepsilon_j}$. Actually, the squeeze film pressure was related with $\vec{\varepsilon}_j$ and $\dot{\vec{\varepsilon}}_j$. This showed that SFD was the special form of SFD/VMR.

On the basis of a short bearing approximation(eq. (8)), and π-film unpressurized oil supply, the squeeze film force are obtained

$$\begin{cases} P_r=\dfrac{\mu R_j L^3}{C^2}(\dot{\varepsilon}I_3+\varepsilon\Omega I_1) \\ P_t=\dfrac{\mu R_j L^3}{C^2}(\dot{\varepsilon}I_1+\varepsilon\Omega I_2) \end{cases} \quad (9)$$

where

$$\left.\begin{aligned} I_1 &= \int_{\theta_1}^{\theta_2} \frac{\sin\theta\cos\theta}{(1+\varepsilon\cos\theta)^3} d\theta = \int_{\pi}^{2\pi} \frac{\sin\theta\cos\theta}{(1+\varepsilon\cos\theta)^3} d\theta = \frac{2\varepsilon}{(1-\varepsilon^2)^2} \\ I_2 &= \int_{\theta_1}^{\theta_2} \frac{\sin^2\theta}{(1+\varepsilon\cos\theta)^3} d\theta = \int_{\pi}^{2\pi} \frac{\sin^2\theta}{(1+\varepsilon\cos\theta)^3} d\theta = \frac{\pi}{2(1-\varepsilon^2)^{1.5}} \\ I_3 &= \int_{\theta_1}^{\theta_2} \frac{\cos^2\theta}{(1+\varepsilon\cos\theta)^3} d\theta = \int_{\pi}^{2\pi} \frac{\cos^2\theta}{(1+\varepsilon\cos\theta)^3} d\theta = \frac{\pi(1+2\varepsilon^2)}{2(1-\varepsilon^2)^{2.5}} \end{aligned}\right\}$$

Referring to Eq. (9) ,the squeeze film stiffness and squeeze film damping of SFD/VMR for circular centered orbits can be expressed as

$$\begin{cases} k_0 = -\dfrac{\vec{P}_r}{e} = \dfrac{\mu\Omega R_j L^3}{C^3} \dfrac{2\varepsilon}{(1-\varepsilon^2)^2} \\ d_0 = -\dfrac{\vec{P}_t}{e\Omega} = \dfrac{\mu R_j L^3}{C^3} \dfrac{\pi}{2(1-\varepsilon^2)^{1.5}} \end{cases} \tag{10}$$

3.2 Characteristics of The Squeeze film force of the SFD/VMR

This section researched characteristics of squeeze film force of the SFD/VMR by using numerical calculation, Referred to Eq. (8), Eq. (9) and Eq. (10).And the results of the SFD/VMR and SFD were correspondingly compared and analyzed. About the information of dynamic analysis of damper and relative equation deductions, please refer to reference [9].

The $\varepsilon_j, \varepsilon_b, \varepsilon, k_0, d_0$ and d_0/k_0 of rigid rotor system with SFD or SFD/VMR vs. δ was given from Fig.5 to Fig.8. When the squeeze film was the thinnest, the three dimensions distribution of squeeze film pressure of SFD and SFD/VMR was showed in Fig.9~Fig.10.

The data was selected to calculate the squeeze film force as follows:

Bearing parameter B=0.18

dimensionless stiffness of the VMR K_b =1

loss factor of the VMR η =0.25

Unbalance parameter U=0.2 (be showed in every Fig.5 (a)~Fig.10 (a)) and U=*0.5*(be showed in every Fig.5 (b)~ Fig.10 (b))

From every figure (a), showed: In terms of SFD/VMR, when U=*0.2*, δ =1.1, maximum eccentricity ratio(ε_j=0.6、ε=0.48、ε_b=0.17) occurred, and ε gradually stabilized at about 0.2 . While, when δ =1.3, the maximum eccentricity ratio of SFD ($\varepsilon = \varepsilon_j = 0.54$) occurred, and it gradually stabilized at about 0.22. Comparing with the SFD, the critical speed of the system with SFD/VMR was lower, and ε_j was bigger because the equivalent stiffness of the rotor system was lower, after elastic VMR replaced the stiffing squeeze film ring. The ε decided the distribution of squeeze film pressure. The maximum of ε of SFD/VMR decreased 11 percent, therefore, k_0 decreased *47 percent*, d_0 reduced *30 percent*, but d_0/k_0 increased 33 percent, comparing with SFD. This suggested that SFD/VMR was very effective to the passive regulation of film clearance.

All above indicated that both of SFD/VMR and SFD could worked well, but compared with SFD, SFD/VMR had the better distribution rule of film pressure and characteristics of squeeze film force, when the unbalance was smaller（U= 0.2）.

It can be seen from every figure (b): SFD/VMR could still work stably; when U increased to 0.5; the maximum eccentricity ratio(ε_j=0.95、ε=0.66、ε_b=0.44) were occurred, where δ =1.25. In the same parameter, the value (ε 、 k_0 、 d_0) of SFD could nonlinearly increase with increase of δ , and the typical bistable jump up was happened. Because the unbalance force of SFD system was too large, the squeeze film force presented high nonlinearity with the increase of the rotor speed.

A matter was worthy of note that both the curve of d_0/k_0 of SFD/VMR and the curve of SFD could drop with increasing of δ . But curve of d_0/k_0 of SFD/VMR was on the top of the curve of d_0/k_0 of SFD, as shown in Fig.8.

All above showed that under the bigger unbalance parameter（U=0.5）, the SFD/VMR could passively regulate the film clearance with the changing of squeeze film force, which improved the high nonline of squeeze film force, and avoided the happening of nonlinear vibration such as bistable jump up. Therefore, SFD/VMR was one better damper, which could reduce vibration effectively in the more unbalance range.

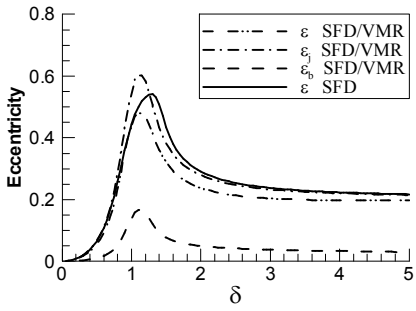

(a) *U*=0.2

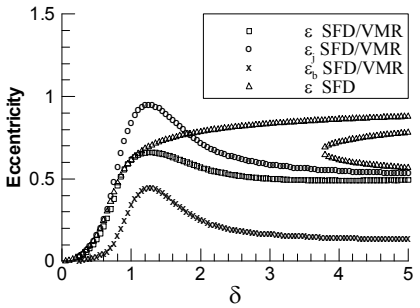

(b) *U*=0.5

Fig.5 The Variation of eccentricity with the change of δ (*B*=0.18, K_b =1, η =0.25)

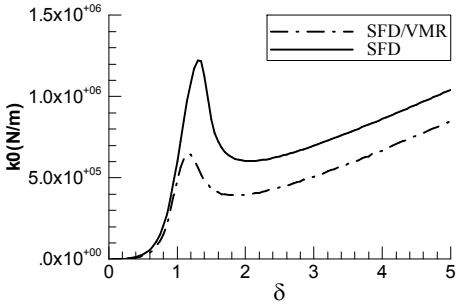

(a) *U*=0.2

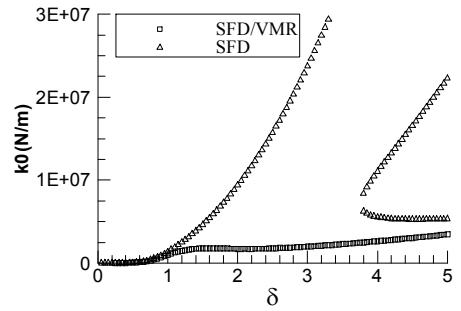

(b) *U*=0.5

Fig.6 The Variation of k_0 with the change of δ (*B*=0.18, K_b =1, η =0.25)

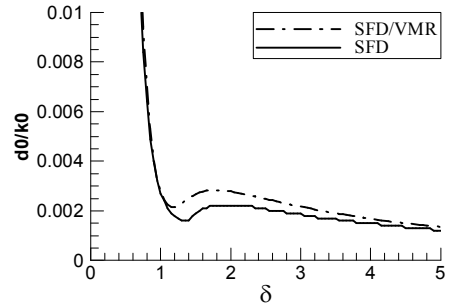

(a) *U*=0.2

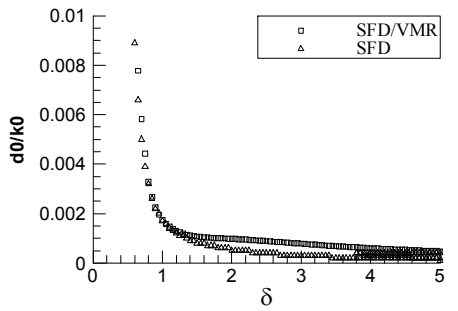

(b) *U*=0.5

Fig.8 The Variation of d_0/k_0 with the change of δ (*B*=0.18, K_b =1, η =0.25)

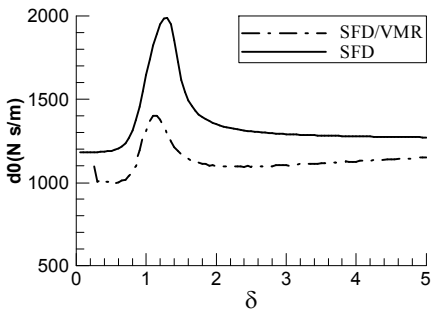

(a) *U*=0.2

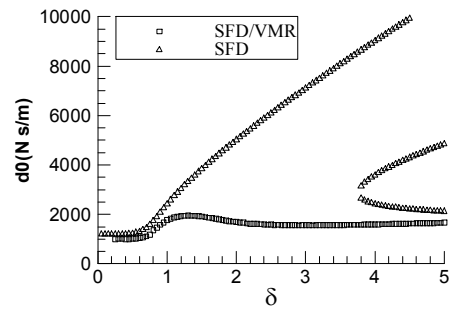

(b) *U*=0.5

Fig.7 The Variation of d_0 with the change of δ (*B*=0.18, K_b =1, η =0.25)

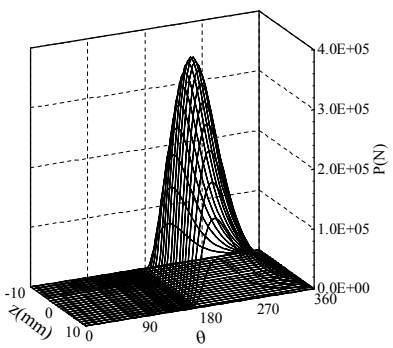

(a)U=0.2

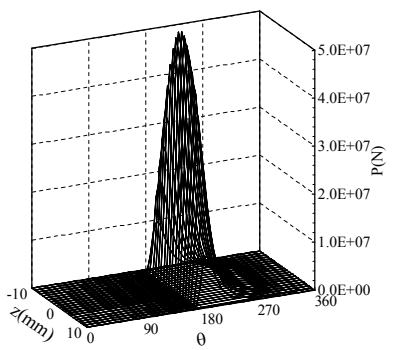

(b) *U*=0.5

Fig.9 The film pressure distributing of three dimensions of the SFD (*B*=0.18, K_b =1, η =0.25)

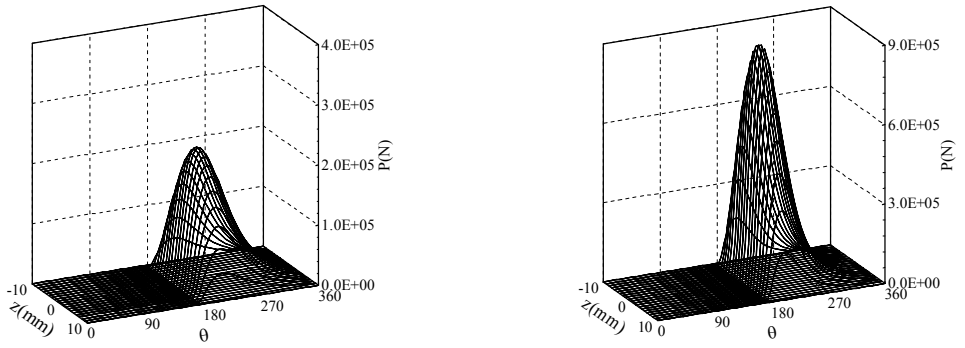

(a) U=0.2 **(b) U=0.5**

Fig.10 The film pressure distributing of three dimensions of the SFD/VMR (B=0.18, K_b =1, η =0.25)

4 EXPERIMENTAL INVESTIGATION

4.1 Rotor Test Rig and Measure System

In this paper, the rigid rotor and measure system were built in test rig, as shown in Fig.11. The test system consisted of DC driver electromotor of 30*KW* and an accelerator (accelerated ratio is 11.05). The maximum speed of the system was 30000*r/min*. Stiffness supporting was designed on one side that was close to the electromotor, absorber supporting was designed on the other side. The absorber included SFD and SFD/VMR. The aim of the experiment was to compare the characteristics of restraining vibration between two absorbers.

Four proximity displacement probes were fixed to measure the vibration signal of journal and squeeze film ring in the x and y directions. Data acquisition and signal processing system of DASP was used to record and analyze, as the test instrument. Due to the restriction to the length of this paper, only the curve of displacement response in the horizontal direction was represented.

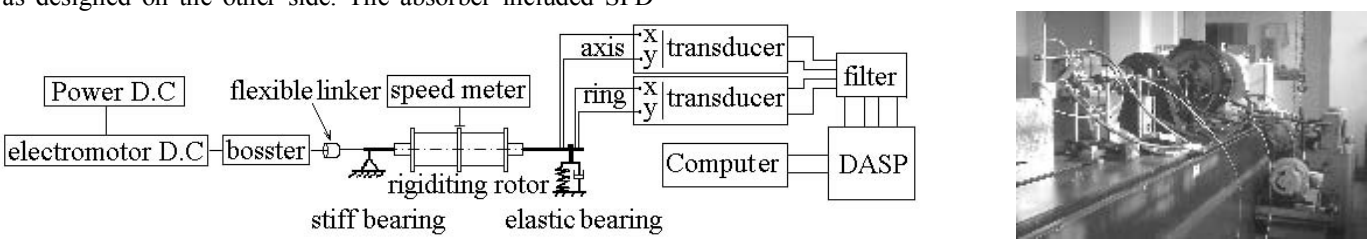

(a) sketch map **(b) practical picture**

Fig.11 Rigid rotor and measure system

For open-ended dampers, the oil pressure was 1 kg/cm^2 in the test, which approximated the environment pressure. The viscosity was 1.884*E-02Pa·s*. The weight of equivalent mass lumped at the bearing station *m=7.3 kg*; the damper radial clearance *c=0.15mm*; the squirrel-cage retainer spring stiffness $k_s = 8.05\times10^5 N/m$; the journal radius R_j =*40mm*; the journal length *L=20mm*; the calculation bearing parameter *B=0.3*. Parameters of the VMR were given Table 1.

outer diameter of the VMR	*OD*	=	*100*	*mm*
inner diameter of the VMR	*ID*	=	*86*	*mm*
axle width of the VMR	*l*	=	*21*	*mm*
wire diameter of the VMR	d_s	=	*0.13*	*mm*

Table 1 Parameters of the VMR

Representative experimental results of static stiffness of the VMR were given in Fig.12(a). When the displacement was small, the curve of static stiffness of valvular metal rubber nearly nonlinear-changed, and with the augment of displacement, nonlinear characteristics could gradually boost up. In this test, the rotor amplitude was smaller, therefore, the valvular metal rubber worked in the linear stage. The result of line-simulated to the stage of small deformation of curve in Fig.12 (a) was showed Fig.12 (b).

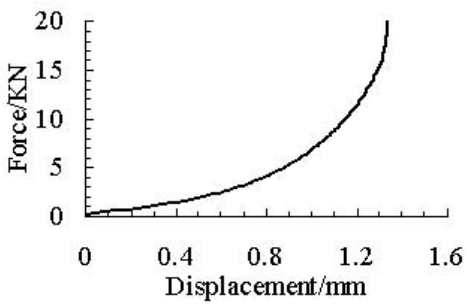

(a) Experimental results of static stiffness of the VMR

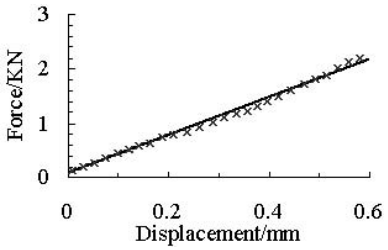

(b) The result of line-simulated

Fig.12 Curve of static rigidity of VMR

4.2 Investigation of Reduction Vibration Validity

Eccentricity response curves of rigid rotor system with SFD and SFD/VMR were respectively shown in Fig.13 and Fig.14 which were in the same test conditions and the same damper parameters. Due to large bearing parameter *B*, it can be seen from Fig.13 that under bigger unbalance, U=0.36 and U=0.55, the SFD system could pass through the first critical speed in a smaller ε. But ε increased quickly with the increase of *U*. And under U=0.6, the bistable jump up occurred within rotor speed range ω =105～130Hz. .

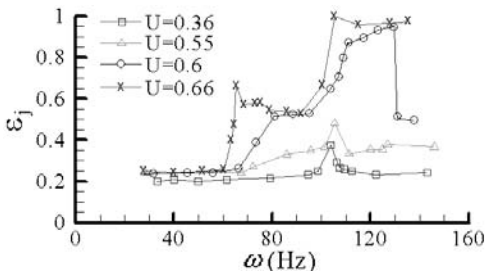

Fig.13 Response of Rigid rotor system with SFD

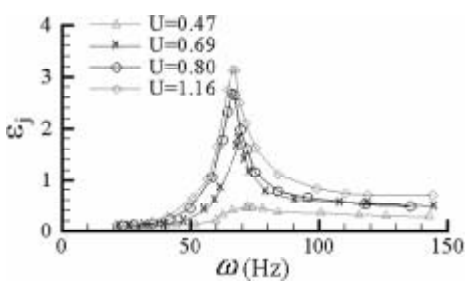

(a)Journal of SFD/VMR

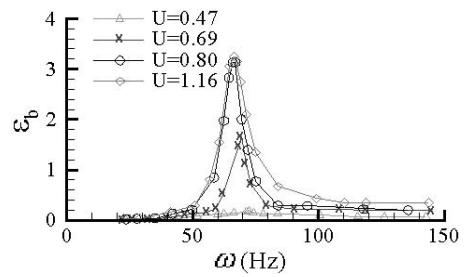

(b) Squeeze film ring of SFD/VMR

Fig.14 Response of Rigid rotor system with SFD/VMR

The comparison between the figure13 and figure14 showed:

1. The SFD/VMR system could stably pass through critical speed, and the nonlinear behavior was not apparent under the unbalance parameter from U=0 to U=1.06; which meant the unbalance range SFD/VMR could support （$U<1.16$） was about twice of SFD （$U<0.55$）, and SFD/VMR could make a better job in restraining the nonlinear vibration such as bistable jump up.

2. Under normal unbalance U<0.36, The critical peak value of ε_j of SFD/VMR was smaller than SFD's, which meant SFD/VMR kept the better characteristics of reducing vibration, when the unbalanced force was small. Under larger unbalance U>0.6, critical peak value of ε_j of SFD/VMR was bigger than SFD's, because the squeeze film ring of SFD was immovable, which restrained amplitude of journal . ε_j or ε （$\varepsilon_j=\varepsilon$）of SFD can never beyond 1, but sometimes many disadvantaged phenomenon would happen such as bistable jump up and lock up , because the squeeze film was too thin. The squeeze film ring of SFD/VMR could press the elastic metal rubber. Therefore, ε_j of SFD/VMR could beyond 1, but the clearance of squeeze film could be controlled in a small range (see figure 15).

3. The critical speed of SFD/VMR was lower than the SFD's, because the equivalent supporting stiffness of SFD/VMR system was lower than the SFD system's. In this example, the critical speed of SFD was between 100Hz and 108Hz. While the critical rotor speed of SFD/VMR was between 64Hz and 70Hz.

4. The rigidity rotor system of SFD showed its hard characteristics. As the figure13 showed, the critical peak value point moved to the high rotor speed range with the increase of U. And the reason was that the increase of ε of SFD lead to the increase of squeeze film stiffness, then the systemic equivalent supporting stiffness increased. The SFD/VMR system showed linearity or soft characteristics. The critical peak value of the system kept itself immovable or moved a little to the region of low speed with the increase of U, which was decided by the material characteristics of Metal Rubber. For avoiding the happening of the high nonlinear phenomenon of rotor system, we often make the Metal Rubber working in the part of linearity or the part of soft characteristics, when we design it, which can make the rotor system pass though the critical speed accelerative.

The Fig 15 showed the changing curve of the dimensionless least film thickness $H=h_{\_\min}/R_j$ of SFD/VMR system, when the unbalances were Q=43.7、66.6、115.4、182.3g cm（U=0.7、1.1、1.8、2.9）.

It can been seen from Fig 15, the film thickness was not sensitive to the change of unbalance and rotor speed; actually, during the rotor system was vibrating in a certain unbalanced range, the film thickness was waving in a small range. Therefore, the elasticity and damping effect of valvular metal rubber could make SFD/VMR passively and self-adaptively regulate the film clearance with the change of squeeze film force, which could make the film thickness of damper keep on waving in a small range. This was identical with the analysis

conclusion.

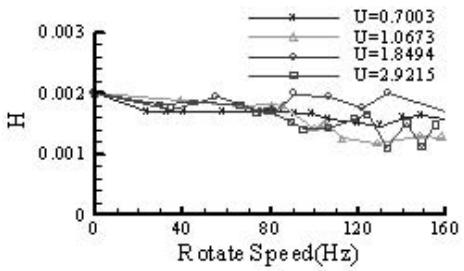

Fig.15 Changing curve of film thickness

5 CONCLUSION

In this paper, a new-style squeeze film damper known as SFD/VMR was designed by taking advantage of the Metal Rubber. And the characteristics of reducing vibration were researched deeply. The theoretical analysis and experimental results identically showed:

(1) SFD/VMR had a very prominent reducing effect in the bigger unbalance range (usually, the unbalance range was the twice of SFD under the same parameter). It could make the rotor system operate more stably and credibly, and could restrain the happening of nonlinear vibration such as bistable jump up, etc.

(2) SFD/VMR possessed the "self-adaptive" capability. Due to the effect of elasticity and damping of valvular metal rubber, SFD/VMR could passively regulate the clearance of squeeze film, which could improve the high nonlinear characteristics. Therefore, the film thickness of SFD/VMR was not very sensitive to the change of unbalance and rotor speed. Actually, the film thickness was waving in a small range during the rotor system was vibrating in a certain unbalance range.

(3) SFD/VMR had the regulating function to critical speed of rotor system. The equivalent stiffness of rotor system would be changed through changing the stiffness of the VMR. Usually, the critical speed of SFD/VMR system was lower than SFD system.

In addition, there were some things need to point out. The stiffness of the VMR had an optimal range to the relative designed parameter of damper. SFD/VMR was able to reduce the vibration effectively, only in this range. This section will be researched in another reference.

6 ACKNOWLEDGMENT

This work was financially supported by the China Aviation Science Foundation 02C51001.

7 REFERENCES

[1] Yan Litang, Zhu Zigen, Song Zhaohong, et al., 1989, "Dynamical characteristic analyse of configuration system," Beijing, Beijing University of Aeronautics and Astronautics Press.

[2] Zhang Shiping, Yan Litang. Development of an efficient squeeze film damper for improving the control of rotor vibtation[J]. Journal of Engineering for Gas Turbines and Power. 1991, 113: 557-562.

[3] David P., Fleming Dual. Clearance Sqeeze Film Damper for High Loadd Conditions[J]. ASME Journal of Tribology. 1985, 107: 275-279.

[4] H. Hooshang, J. F. Walton. Advanced Multi-Sqeeze Film Damper for Rotor Vibration Control[C]. STLE Trib. Tran. 1991, 34:489-496.

[5] Zhu Changsheng, Wang Xixuan, "Vibration Control of Flexible Rotor by Controlled Structure Parameters Conical Squeeze Film Damper," Journal of Zhejiang University, 1994, Vol.28, No.6, pp. 613-621.

[6] Zhu Changsheng, Wang Xixuan, "Vibration control of flexible rotor by hybrid squeeze film damper," Journal of Mechanical Engineering, 1996, Vol.32 No.3.pp. 76-83

[7] Zhou Ming, Li Qihan, 1996, "Theoretical and experimental investigation on the elastic ring squeeze film damper", Ph.D. thesis, Dept of Propulsion, Beijing University of Aeronautics and Astronautics.

[8] Zhao Jie, Yan Litang, 1997, "Theoretical and experimental investigation on the movable outer-ring squeeze film damper," Dept of Propulsion, Beijing University of Aeronautics and Astronautics.

[9] Ma Yanhong, Hong Jie, 2002, "Experimental investigation of a adaptive squeeze film damper with metal rubber outer-ring," Master's thesis, Dept of Propulsion, Beijing University of Aeronautics and Astronautics.

[10] Zarzour. M., Vance. J. M., "Experimental evaluation of a metal mesh bearing damper," ASME Journal of Engineering for Gas Turbines and Power. 2000, Vol.122, pp. 326-329

[11] Al-Khateeb. E., Vance. J. M., "Experimental Evaluation of a Metal Mesh Damper In Parallel With a Structural Support," ASME Paper No.2001-GT-0247.

[12] Shen Xinmin, Wen Yingmei, Sun Xitong, et al. 1991, "Foundations of Tribology ," Beijing, Beijing University of Aeronautics and Astronautics Press. pp. 40-49.

[13] Ocvirk. F. W. and DuBois. G. B. Analytical derivation and experimental evaluation of short bearing approximations of full journal bearings. 1953, Report 1157, NACA.